Radiative Signatures From The Cosmos
ASP Conference Series, Vol. 519
K. Werner, C. Stehlé, T. Rauch, and T. M. Lanz, eds.

Spectral Analysis of Binary Pre-white Dwarf Systems

N. L. Finch,[1] I. P. Braker,[1] N. Reindl,[1] M. A. Barstow,[1] S. L. Casewell,[1] M. Burleigh,[1] T. Kupfer,[2] D. Kilkenny,[3] S. Geier,[4] V. Schaffenroth,[4] M. M. Miller Bertolami,[5] S. Taubenberger,[6] and J. Freudenthal[7]
[1]*University of Leicester, Leicestershire, England;* [2]*University of California, Santa Barbara, CA, USA;* [3]*University of the Western Cape, Bellville, Cape Town, South Africa;* [4]*Universität Potsdam, Golm, Potsdam, Germany;* [5]*Instituto de Astrofísica de La Plata, La Plata, Beunos Aires, Argentina;* [6]*Max Planck Institut für Astrophysik, Garching, Germany;* [7]*Institut für Astrophysik Göttingen, Göttingen, Germany;*

Abstract. Short period double degenerate white dwarf (WD) binaries with periods of less than ~1 day are considered to be one of the likely progenitors of type Ia supernovae. These binaries have undergone a period of common envelope evolution. If the core ignites helium before the envelope is ejected, then a hot subdwarf remains prior to contracting into a WD. Here we present a comparison of two very rare systems that contain two hot subdwarfs in short period orbits. We provide a quantitative spectroscopic analysis of the systems using synthetic spectra from state-of-the-art non-LTE models to constrain the atmospheric parameters of the stars. We also use these models to determine the radial velocities, and thus calculate dynamical masses for the stars in each system.

1. Introduction

Double degenerate systems with short enough orbits and high enough system masses are candidates for type Ia supernovae (SN Ia), via the proposed double degenerate merger channel (Webbink 1984). Double degenerates will spiral inwards due to the emission of gravitational waves, but for this to occur in a Hubble lifetime requires periods of less than ~1 day. There are ~100 double WD binaries (Brown et al. 2017), as well as ~50 known WD-hot subdwarf binaries (Kupfer et al. 2015) with such periods; however, there are only a few double hot subdwarf systems (Ahmad et al. 2004; Lisker et al. 2004). Of these double degenerates, only a handful are of sufficient mass to be considered SN Ia candidate systems. Hot subdwarfs are the stripped cores of red giants, usually surrounded by a thin H-layer. They are either core or shell burning, and when this ceases they will contract towards the WD cooling curve. Many hot subdwarfs are found in binary systems, suggesting that they lost their envelope through interactions with the secondary star. It has also been suggested that single hot subdwarfs are the product of the merger of two He-core WDs (Webbink 1984). Hot subdwarfs have often been found with WD or low mass stellar companions, but rarely with another hot subdwarf. A double hot subdwarf system provides constraints on the binary evolution channels of these objects. Eclipsing binaries and binaries with known inclination are especially useful, as they allow us to determine the masses and radii of each component for characterising the system.

Santander-Garcia et al. 2015 identified a potential double hot subdwarf system within Hen 2-428, a known planetary nebula. The system is not eclipsing but does show high amplitude sinusoidal variation due to the over contact nature of the central stars. Santander-Garcia et al. 2015 determined masses from the light curve fitting which suggested the system is a SN Ia progenitor. However, the analysis of the spectra of Hen 2-428 (Finch et al. 2018; Reindl et al. 2018; Finch et al. 2019) suggests lower masses, insufficient to produce a SN Ia.

In the following sections we summarise our spectroscopic analysis of Hen 2-428. We also present the preliminary analysis of a new eclipsing hot subdwarf binary system, SDSS J135713.14-065913.7 (SDSS 1357-0659), and then discuss how the initial analysis of this system compares to Hen 2-428.

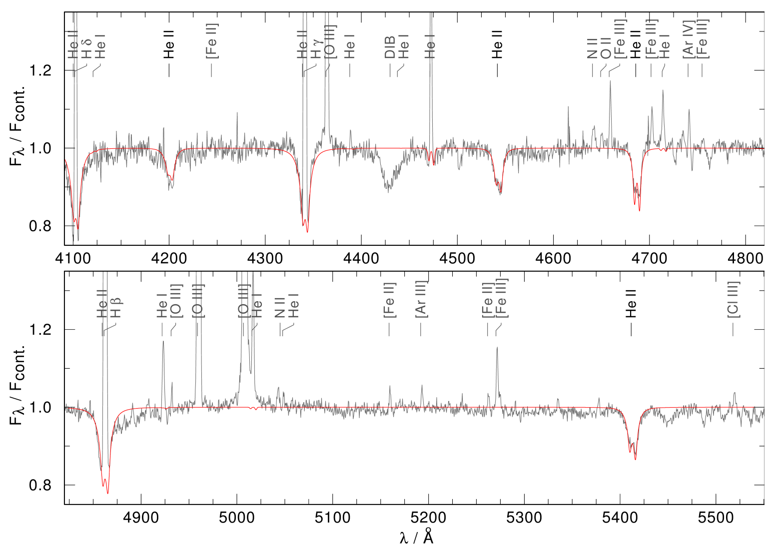

Figure 1. GTC spectrum (grey) of Hen 2-428 showing the best fitting model overlaid (red). Four He II lines (black) were used for the fitting.

2. Overview of Hen 2-428

Fig. 1 shows a GTC/OSIRIS spectrum of Hen 2-428. We identify four He II lines (4200, 4542, 4686 and 5412 Å), each a superposition of two photospheric absorption features, one from each star. There are also many nebula emission lines, some of which are contaminating the hydrogen Balmer series.

We employ the Tübingen Model Atmospheres Package (TMAP: Werner et al. 2003, Rauch and Deetjen 2003, Werner et al. 2012) to create non-LTE model atmospheres as described in Reindl et al. 2018 and Finch et al. 2019. When fitting the model spectra to observations, we use a chi square minimisation code, XSPEC (Arnaud 1996), with necessary conversions to allow compatibility with optical spectra (Dobbie et al. 2004). First the radial velocity of each component was found, then the flux contribution, $T_{\rm eff}$, $\log g$ and $\log\,(n_{\rm He}/n_{\rm H})$ were constrained simultaneously.

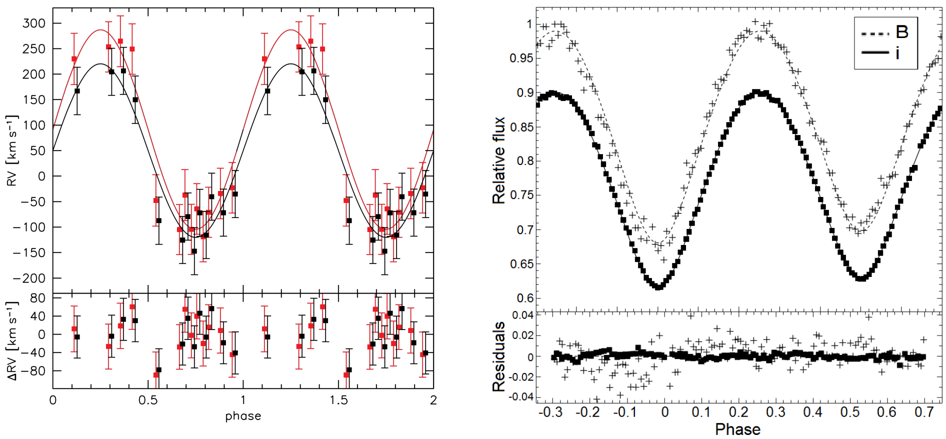

Figure 2. *Left:* Radial velocity curves from one of the stars, for 4686 Å and 5412 Å (black and red, respectively). *Right:* Light curve data from Santander-Garcia et al. 2015 fitted using MORO.

We provide spectroscopic parameters from the fitting of one of the available spectra, which had good S/N and where the absorption lines were well separated by radial velocity. The best fit model and spectrum are shown in Fig. 1, where model parameters are 49.7 ± 7.0 kK, log g of 5.0 ± 0.3 and helium abundance (n_{He}/n_H) of 0.08 for the first star. For the second star the parameters constrained are 45.4 ± 7.6 kK, log g of 4.7 ± 0.2 and helium abundance of 0.09. Flux contributions are 48.7% and 51.3% respectively. The built-in error analysis function STEPPAR was used to constrain the 1σ errors.

Detailed radial velocity analysis for Hen 2-428 can be found in Reindl et al. 2018 and Finch et al. 2019, so here we briefly summarise. Radial velocities were found by fitting the synthetic spectra to all four He II lines, to just the 4686 Å line, and to just the 5412 Å line. Of the individual lines, the latter has a greater radial velocity amplitude and thus produces higher dynamical masses. Fig. 2 illustrates this amplitude difference. A cause for this is yet to be definitively shown. The dynamical masses, as taken from an analysis of all available lines, are $0.51 \pm 0.11\,M_\odot$ and $0.51 \pm 0.10\,M_\odot$.

Fig. 2 also shows the light curve fitting, using the data from Santander-Garcia et al. 2015 and the code MORO (Drechsel et al. 1995). Temperatures from the spectral analysis, which are ~16 kK greater than those given in Santander-Garcia et al. 2015, are used as initial parameters. The figure shows that higher temperature, and lower mass, objects can fit the light curve data equally well.

3. Analysis of SDSS 1357-0659

We subsequently identified a hot subdwarf binary system which is eclipsing (Braker et al. *in prep*). The eclipse depths are similar with little evidence of sinusoidal variability (Fig. 3), suggesting similar mass stars with similar temperatures. One component had been previously identified as a hot subdwarf (Baxter et al. 2014), suggesting this is potentially the first known eclipsing double hot subdwarf system.

17 VLT/FORS2 observations were obtained of the system, covering two 2.5 hr orbits, from which we identified spectral features from both components (Fig. 4). Double

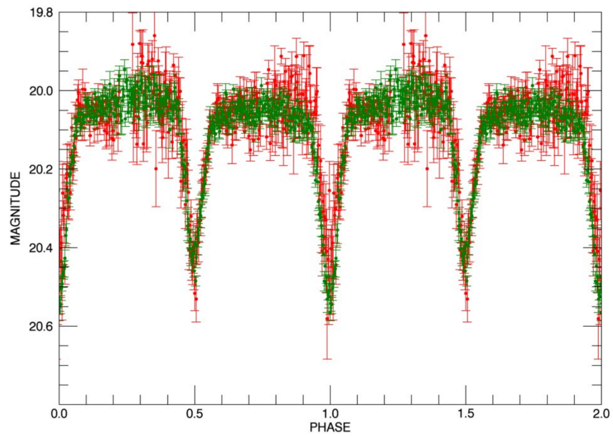

Figure 3. CHIMERA light curves from two bands overlaid for comparison.

lined, photospheric absorption features from the hydrogen Balmer series (Hβ through to H 9) as well as two He I lines (4026 and 4471 Å) and three He II lines (4200, 4542 and 4686 Å) are visible. We also identify a Ca II line at 3933 Å, which is likely contamination from the ISM.

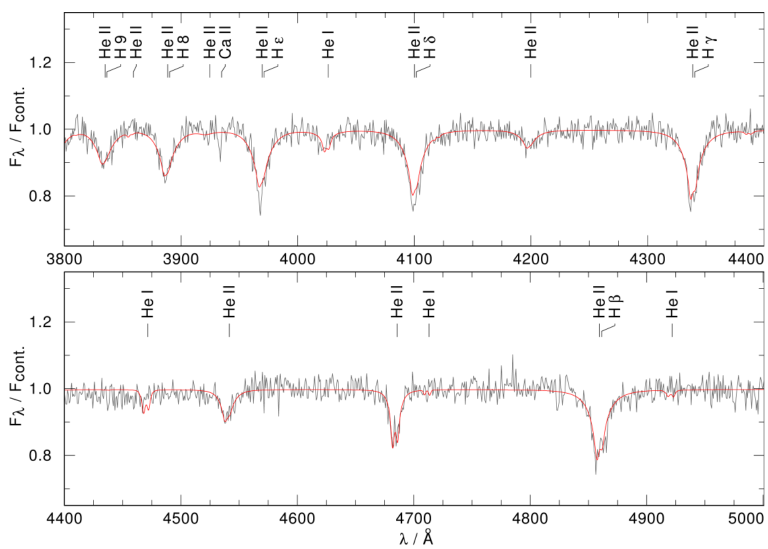

Figure 4. FORS2 spectrum of SDSS 1357-0659 showing the best fitting model overlaid (red).

Again, we use TMAP to model the system, however we use a modified range of surface gravities, 4.50 - 7.00 in 0.25 dex steps. First we found the radial velocity of each component, then the flux contribution, $T_{\rm eff}$, $\log g$ and $\log(n_{\rm He}/n_{\rm H})$ simultaneously.

The best fit model and spectrum are shown in Fig. 4. Model parameters are 47.2 ± 2.8 kK, $\log g$ of 5.43 ± 0.15 and helium abundance ($n_{\rm He}/n_{\rm H}$) of 0.097 for the first star, and 48.3 ± 3.2 kK, $\log g$ of 5.97 ± 0.20 and helium abundance of 0.072 for the second star. Flux contributions are 54% and 46% respectively. The built-in error analysis function STEPPAR was used to constrain the 1σ errors.

Our synthetic spectra were used to produce radial velocity curves for the stars in the system using all available lines. The amplitudes found were $187.5 \pm 5.2\,\mathrm{km\,s^{-1}}$ and $181.7 \pm 10.0\,\mathrm{km\,s^{-1}}$, with corresponding masses of $0.27 \pm 0.05\,\mathrm{M_{\odot}}$ and $0.28 \pm 0.02\,\mathrm{M_{\odot}}$, respectively.

4. Comparison

We have analysed Hen 2-428 and SDSS 1357-0659, and can now compare these systems. We note the similarities between the temperatures and helium abundances of each system. This is to be expected given both systems contain stars which are hot enough to display photospheric He II lines. The surface gravities of SDSS 1357-0659 are higher than for Hen 2-428, suggesting stars with either higher mass or smaller radii for the eclipsing system. The differences in the dynamical masses of each system are striking. For Hen 2-428 masses of $0.51 \pm 0.11\,\mathrm{M_{\odot}}$ and $0.51 \pm 0.10\,\mathrm{M_{\odot}}$ were concluded from the radial velocity curves. Meanwhile, the stars in the eclipsing system are $0.27 \pm 0.05\,\mathrm{M_{\odot}}$ and $0.28 \pm 0.02\,\mathrm{M_{\odot}}$. Therefore, these stars must have smaller radii than the stars in Hen 2-428 in order to produce higher surface gravities.

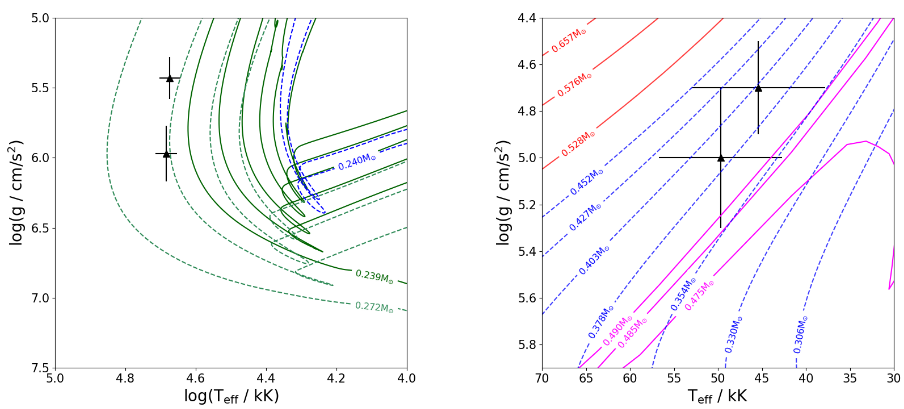

Figure 5. Temperature against surface gravity plots *Left:* showing parameters of the stars in the eclipsing system against tracks from Althaus et al. 2013 and Hall et al. 2013 in green and blue respectively; *Right:* showing parameters for Hen 2-428 with tracks from Miller Bertolami 2016, Hall et al. 2013 and Dorman et al. 1993 in red, blue and magenta respectively.

Fig. 5 shows the spectral parameters plotted in the T_{eff}-log g plane for each system against relevant evolutionary tracks. We must be cautious when applying these tracks to the Hen 2-428 stars, as they are in over-contact, for which the tracks were not designed. The evolution tracks indicate that the stars in Hen 2-428 could be AGB-manqué stars, whilst the dynamical masses do not allow us to distinguish whether one (or both) stars are post-AGB (red) or post-RGB (blue dashed) stars. Potentially, one of them could be a post-EHB (magenta) star. Meanwhile, SDSS 1357-0659 appears most likely to consist of low mass stars undergoing hydrogen flashes (green), thus receiving an increase in temperature for that part of its evolution. However, this evolutionary stage is very short lived, around 10^5 yrs (Istrate et al. 2016). To find two hot subdwarfs in the same system at almost the exact same point on the evolutionary track is hence highly unlikely.

5. Conclusions

We summarise the results from the first spectral analysis of Hen 2-428, and present the initial analysis of the first eclipsing double hot subdwarf. Further work is needed on Hen 2-428 in order to discover the cause of line dependent radial velocity amplitudes.

Acknowledgments. NLF is supported by an STFC studentship. IPB acknowledges support from the University of Leicester College of Science and Engineering and Leicester Institute for Space and Earth Observation (LISEO). NR is supported by a Royal Commission 1851 research fellowship.

References

Ahmad, A., Jeffery, C. S., Fullerton, A. W. 2004, A&A, 418, 275-281
Althaus, L. G., Miller Bertolami, M. M., Córsico, A. H. 2013, A&A, 557, A19
Arnaud, K. A. 1996, Astronomical Society of the Pacific Conference Series, 101, 17
Baxter, R. B., Dobbie, P. D., Parker, Q. A., Casewell, S. L., Lodieu, N., Burleigh, M. R., Lawrie, K. A., Külebi, B., Koester, D., Holland, B. R. 2014, MNRAS, 440, 3184-3201
Brown, W. R., Kilic, M., Kosakowski, A., Gianninas, A. 2017, ApJ, 847, 10
Dobbie, P. D., Pinfield, D. J., Napiwotzki, R., Hambly, N. C., Burleigh, M. R., Barstow, M. A., Jameson, R. F., Hubeny, I. 2004, MNRAS, 355, L39-L43
Dorman, B., Rood, R. T., O'Connell, R. W. 1993, ApJ, 419, 596
Drechsel, H., Haas, S., Lorenz, R., Gayler, S. 1995, A&A, 294, 723-743
Finch, N. L., Reindl, N., Barstow, M. A., Casewell, S. L., Geier, S., Miller Bertolami, M. M., Taubenberger, S. 2018, Open Astronomy, 27, 57-61
Finch, N. L., Reindl, N., Barstow, M. A., Casewell, S. L., Geier, S., Schaffenroth, V., Miller Bertolami, M. M., Taubenberger, S. 2019, University of Texas Libraries, https://repositories.lib.utexas.edu/handle/2152/71506
Hall, P. D., Tout, C. A., Izzard, R. G., Keller, D. 2013, MNRAS, 435, 2048-2059
Istrate, A. G., Marchant, P., Tauris, T. M., Langer, N., Stancliffe, R. J., Grassitelli, L. 2016, A&A, 595, A35
Kupfer, T., Geier, S., Heber, U., Østensen, R. H., Barlow, B. N., Maxted, P. F. L., Heuser, C., Schaffenroth, V., Gänsicke, B. T. 2015, A&A, 576, A44
Lisker, T., Heber, U., Napiwotzki, R., Christlieb, N., Reimers, D., Homeier, D. 2004, Ap&SS, 291, 351-358
Miller Bertolami, M. M. 2016, A&A, 588, A25
Rauch, T., Deetjen, J. L. 2003, Astronomical Society of the Pacific Conference Series, 288, 103
Reindl, N., Finch, N., Schaffenroth, V., Barstow, M., Casewell, S., Geier, S., Miller Bertolami, M., Taubenberger, S. 2018, Galaxies, 6, 88
Santander-García, M., Rodríguez-Gil, P., Corradi, R. L. M., Jones, D., Miszalski, B., Boffin, H. M. J., Rubio-Díez, M. M., Kotze, M. M. 2015, Nature, 519, 63-66
Werner, K., Deetjen, J. L., Dreizler, S., Nagel, T., Rauch, T., Schuh, S. L. 2003, Astronomical Society of the Pacific Conference Series, 288, 31
Werner, K., Dreizler, S., Rauch, T. 2012, Astrophysics Source Code Library
Webbink, R. F. 1984, ApJ, 277, 355-360